Solid State Communications 150 (2010) 157–159

Contents lists available at ScienceDirect

Solid State Communications

journal homepage: www.elsevier.com/locate/ssc

Giant magnetocaloric effect in HoGa compound over a large temperature span

J. Chen [a], B.G. Shen [a,*], Q.Y. Dong [b], J.R. Sun [a]

[a] State Key Laboratory for Magnetism, Institute of Physics, Chinese Academy of Sciences, Beijing, 100190, People's Republic of China

[b] Department of Physics, Capital Normal University, Beijing, 100048, People's Republic of China

ARTICLE INFO

Article history:
Received 14 September 2009
Accepted 18 October 2009
by A.H. MacDonald
Available online 21 October 2009

PACS:
71.20.Eh
75.50.Cc
75.30.Sg

Keywords:
C. CrB-type structure
D. Magnetocaloric effect
D. Spin-reorientation transition

ABSTRACT

We have studied experimentally the magnetic properties and magnetocaloric effect (MCE) in HoGa compound. Two subsequent magnetic transitions, a spin-reorientation (SR) transition followed by a ferromagnetic (FM)–paramagnetic (PM) transition, are observed at $T_{SR} \sim 20$ K and $T_C \sim 69$ K, respectively. Both transitions contribute greatly to the magnetic entropy change (ΔS_M), each yielding a significant peak on their ΔS_M–T curve. A considerable value of refrigerant capacity (RC) is obtained in HoGa, due to the large MCE over a wide temperature span. For a magnetic field change of 0–5 T, the maximal values of $-\Delta S_M$ are 17.1 J/kg K and 7.8 J/kg K at T_C and T_{SR}, respectively, and the RC reaches its maximal value of 455 J/kg in an optimal reversible refrigerant cycle with cold and hot sinks at $T_{\text{cold}} \sim 16$ K and $T_{\text{hot}} \sim 99$ K. Large reversible MCE and the giant value of RC indicate the potentiality of HoGa as a candidate magnetic refrigerant for nitrogen liquefaction.

1. Introduction

Recently, much attention has been paid to studies on the magnetocaloric effect (MCE) of magnetic materials, because the magnetic refrigeration based on MCE is expected to be a promising alternative technology to the conventional gas compression refrigeration due to its higher energy efficiency and friendly environment [1–4]. The MCE is usually characterized by the magnetic entropy change (ΔS_M) and/or adiabatic temperature change (ΔT_{ad}). However, it is not sufficient to identify the potential of a magnetic refrigerant material solely by the large magnetic entropy change (ΔS_M). Another important parameter is the refrigerant capacity (RC), a measure of how much heat can be transferred between the cold and the hot sinks in one ideal refrigeration cycle, which depends on not only the ΔS_M value but also the width of the ΔS_M–T curve. A large number of materials with first-order magnetic transition have been found to exhibit giant MCEs around their transition temperatures [5–14], yet the majority of them are found to possess a much smaller RC than those materials with a second-order magnetic transition, because the first-order transition usually occurs over a relative small temperature range. In addition, the considerable thermal and magnetic hysteresis that is accompanied by the first-order magnetic transition will reduce greatly the actual RC of the materials in a fast-cycling refrigerator. Therefore, it is necessary to explore magnetic materials with a large reversible MCE as well as a wide temperature interval based on the second-order phase transition. Besides, many previously reported materials, such as $Gd_{0.54}Er_{0.46}AlNi$ [15], Gd_4Co_3 [16], and Ho_2In [17], show clearly that multiple magnetic transitions can enlarge the working temperature range effectively and hence enhance the RC significantly, which is desired for optimizing the efficiency of the magnetic Ericsson refrigeration cycles. So it makes sense to explore magnetic materials with several reversible magnetic transitions.

The intermetallic HoGa compound was firstly reported to be a ferromagnet with two magnetic transitions in sequence, a spin-reorientation (SR) transition at $T_{\text{SR}} \sim 10$–22 K and a transition from ferromagnetic (FM) to paramagnetic (PM) states at $T_C \sim 67$ K [18]. Later on, Delyagin et al. revealed that the SR transition in HoGa occurs at $T_{\text{SR}} \sim 18(1)$ K [19]. We carefully investigate the magnetic properties and MCE of HoGa by magnetization measurements. Our results show that HoGa undergoes a SR transition at $T_{\text{SR}} \sim 20$ K followed by a FM–PM transition at $T_C \sim 69$ K, and each transition contributes greatly to the magnetic entropy change (ΔS_M). The giant MCEs over a wide temperature span produce a remarkable RC in HoGa.

2. Experiments

The polycrystalline HoGa compound was prepared by arc melting the constituent elements of purity better than 99.9% in an argon atmosphere. The alloy was turned over and remelted four times to ensure homogeneity. The obtained ingot was wrapped in

* Corresponding author. Tel.: +86 10 82648082; fax: +86 10 82649485.
E-mail address: shenbg@g203.iphy.ac.cn (B.G. Shen).

0038-1098/$ – see front matter © 2009 Elsevier Ltd. All rights reserved.
doi:10.1016/j.ssc.2009.10.023

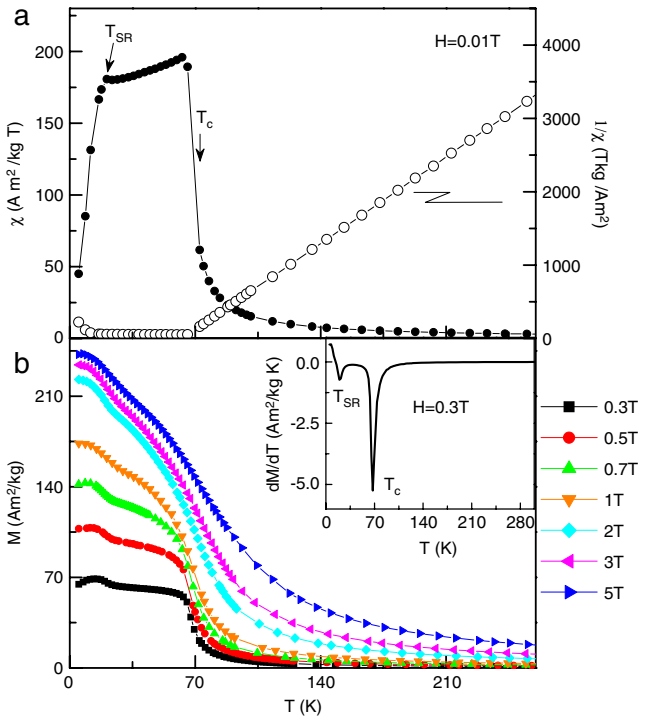

Fig. 1. (Color online) (a) Temperature dependence of zero-field-cooling susceptibility (χ) and the inverse of susceptibility ($1/\chi$) of HoGa at a magnetic field of 0.01 T. (b) Temperature dependencies of magnetization under different magnetic fields. The inset shows the dM/dT curve under a magnetic field of 0.3 T.

a molybdenum foil, sealed in a high-vacuum quartz tube, annealed at 800 °C for one week and then quenched into liquid nitrogen. X-ray diffraction (XRD) measurements on powder samples were performed at room temperature by using Cu Kα radiation to identify the phase structure and the crystal lattice parameters. The magnetization and the heat capacity were measured by employing a physical property measurement system (PPMS) from Quantum Design. The value of ΔS_M was calculated by the Maxwell relation based on magnetization data.

3. Results and disscution

The XRD pattern of HoGa reveals the single-phase nature of the sample, crystallizing in the orthorhombic CrB-type structure (space group Cmcm). The lattice parameters a, b, and c, are determined to be 4.280(9), 10.781(9), and 4.042(4) Å, respectively, by using the Rietveld refinement method. The residual factor R_{wp} is equal to 11.7%. The temperature dependencies of zero-field-cooling susceptibility (χ) and the inverse susceptibility ($1/\chi$) under a low applied field of 0.01 T are shown in Fig. 1(a). A sharp change in susceptibility around T_{SR} is observed in the χ–T curve, corresponding to a SR transition. Another abrupt change around T_C reveals the occurrence of the magnetic transition from FM to PM states. In the paramagnetic region, the susceptibility exhibits a Curie–Weiss behavior. Calculation results show that the effective paramagnetic moment (μ_{eff}) and the Curie temperature (θ_P) are equal to $10.56\mu_B/Ho^{3+}$ and 63 K, respectively. The μ_{eff} value is close to the free ion moment of Ho^{3+} ($10.60\mu_B$). The magnetizations as a function of temperature in various external magnetic fields are displayed in Fig. 1(b). It is found that the magnetization below T_{SR} increases greatly with increasing field, and is nearly unchanged at the applied field $H \geq 2$ T. The SR and FM–PM transitions are clearly observed, as indicated by the stepwise behavior of the M–T curves around the transition temperatures. The transition

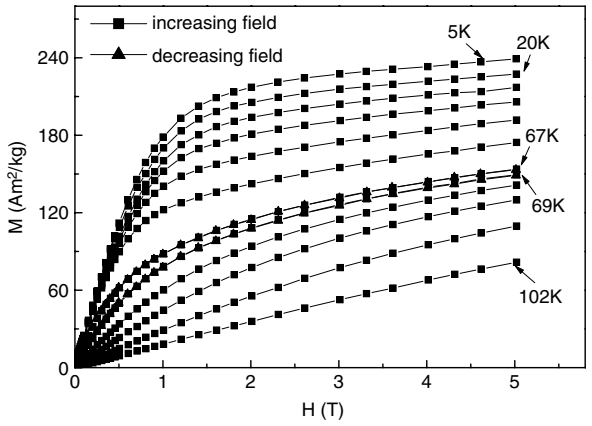

Fig. 2. Magnetization isotherms of HoGa in a temperature range of 5–102 K measured with field increasing (solid squares) and field decreasing (solid triangles) in different temperature steps.

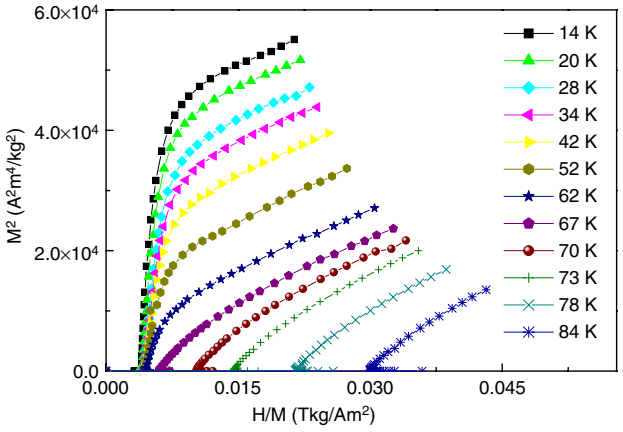

Fig. 3. (Color online) Arrott plots of HoGa from 14–84 K in different temperature steps.

temperatures T_{SR} and T_C are determined to be 20 and 69 K, respectively, by evaluating the dM/dT minima of the M–T curve under a field of 0.3 T. Both the values of T_{SR} and T_C are almost consistent with the results reported by Nesterov et al. [18] and Delyagin et al. [19] based on Mössbauer spectroscopy measurements.

The isothermal magnetization curves as a function of magnetic field were measured in applied fields of up to 5 T in a wide temperature range with different temperature steps as shown in Fig. 2. The sweep rate was slow enough to ensure that the M–H curves could be recorded in an isothermal process. The magnetization increases rapidly at low fields and shows a tendency to saturate with an increase of the field, exhibiting typical FM nature. To investigate the reversibility of the magnetic transitions for HoGa, the M–H curves were measured respectively in field increasing and decreasing modes at 67 and 69 K. Obviously, there is almost no magnetic hysteresis in each curve, indicating the perfect magnetic reversibility of the magnetic transitions in HoGa. The H/M versus M^2 curves, i.e. Arrott plots, from 14–84 K in different temperature steps are plotted in Fig. 3. The positive slopes of plot around T_C confirm that the FM–PM transition in HoGa is of second-order [20].

The magnetic entropy change of HoGa was calculated from magnetization isotherms by using the Maxwell relation $\Delta S_M = \int_0^H (\frac{\partial M}{\partial T})_H dH$ [21,22]. The temperature dependencies of ΔS_M calculated from magnetizations for different magnetic field changes are presented in Fig. 4. Two peaks are found to be centered at T_{SR} and T_C, respectively, corresponding to the double transitions detected clearly in magnetic measurements. The maximal values

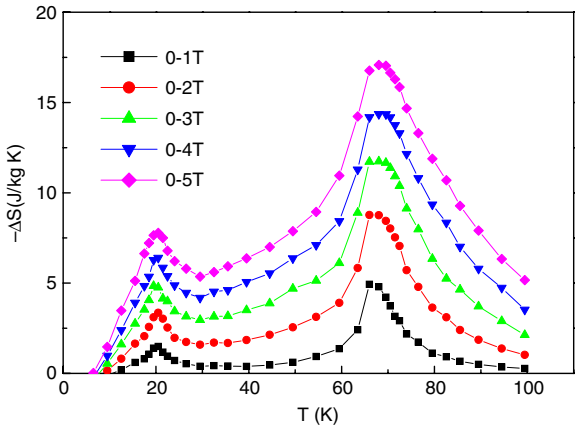

Fig. 4. (Color online) Magnetic entropy change of HoGa as a function of temperature for various field changes of 0–1 T, 0–2 T, 0–3 T, 0–4 T, and 0–5 T, respectively.

Table 1
Comparison of the main parameters regarding the MCE between HoGa and some representative refrigerant materials.

Materials	$-\Delta S_M$ (J/kg K)	RC (J/kg)	T_{cold} (K)	T_{hot} (K)	T_C (K)	Refs.
Ho_2In	11.2	360	16	126	85	[17]
$HoCo_2$	22	216	76	94	78	[25]
TbCoAl	10.5	265	42	95	70	[26]
HoGa	17.1	455	16	99	69	This work

of $-\Delta S_M$ are 7.8 and 17.1 J/kg K at T_{SR} and T_C, respectively, for a field change of 0–5 T. The $-\Delta S_M$ value that is caused by the SR transition has been rarely reported in polycrystalline compounds previously. Only in $HoAl_2$ [23], Gd_4Co_3 [16], and Ho_2In [17] can the SR transition bring a visible peak on each ΔS_M–T curve. It can be seen from Fig. 4 that the two peaks partly overlap between T_{SR} and T_C, which enlarges greatly the temperature range of MCE and produces a nearly constant $-\Delta S_M$, suggesting the possibility to achieve a considerable RC in HoGa.

The RC of HoGa was estimated by using the approach suggested by Wood and Potter [24]. The refrigerant capacity for a reversible refrigeration cycle operating between T_{hot} (the temperature of the hot ends) and T_{cold} (the temperature of the cold ends) is defined as RC $= -\Delta S_M \times \Delta T_{cycl}$, where $-\Delta S_M$ is the magnetic entropy change at the hot and cold ends of the cycle with equal magnitudes, and $\Delta T_{cycl} = T_{hot} - T_{cold}$. Calculations show that the optimum refrigeration cycle occurs between $T_{cold} \sim 16$ K and $T_{hot} \sim 99$ K, with a maximal RC value of 455 J/kg for a magnetic field change of 0–5 T, which is larger than those for $HoCo_2$ (216 J/kg) [25], TbCoAl (265 J/kg) [26] and Ho_2In (360 J/kg) [17] (see Table 1), where the RC values of the former two compounds are estimated from the temperature dependence of ΔS_M in the literature, respectively. Evidently, the large RC of HoGa originates from the combined contribution from SR and FM–PM transitions, which enlarges the temperature span of a large MCE.

4. Conclusions

We have studied experimentally the magnetic and magnetocaloric properties of HoGa, and further calculated its MCE and RC values based on the experimental data. Our results indicate that HoGa possesses a large reversible MCE, characterized by two ΔS_M peaks caused by a SR transition and a FM–PM transition, i.e. $-\Delta S_M = 17.1$ J/kg K at T_C and 7.8 J/kg K at T_{SR} for a field change of 0–5 T. The maximum value of RC is estimated to be as large as 455 J/kg over a wide working temperature range $\Delta T_{cycl} = 83$ K for a field change of 0–5 T. The excellent magnetocaloric performance indicates the applicability of HoGa to the liquefaction of nitrogen gas.

Acknowledgements

This work was supported by the National Basic Research Program of China, the National Natural Science Foundation of China and the Knowledge Innovation Project of the Chinese Academy of Sciences.

References

[1] C.B. Zimm, A. Jastrab, A. Sternberg, V.K. Pecharsky, K.A. Gschneidner Jr., M. Osborne, I. Anderson, Adv. Cryog. Eng. 43 (1998) 1759.
[2] V.K. Pecharsky, K.A. Gschneidner Jr., J. Magn. Magn. Mater. 200 (1999) 44.
[3] A.M. Tishin, Y.I. Spichkin, in: J.M.D. Coey, et al. (Eds.), The Magnetocaloric Effect and its Applications, Institute of Physics Publishing, 2003.
[4] K.A. Gschneidner Jr., V.K. Pecharsky, A.O. Tsokol, Rep. Progr. Phys. 68 (2005) 1479.
[5] V.K. Pecharsky, K.A. Gschneidner Jr., Phys. Rev. Lett. 78 (1997) 4494.
[6] A. Giguere, M. Foldeaki, W. Schnelle, E. Gmelin, J. Phys.: Condens. Matter 11 (1999) 6969.
[7] F.X. Hu, B.G. Shen, J.R. Sun, X.X. Zhang, Chin. Phys. 9 (2000) 550.
[8] F.X. Hu, B.G. Shen, J.R. Sun, Z.H. Cheng, G.H. Rao, X.X. Zhang, Appl. Phys. Lett. 78 (2001) 3675.
[9] H. Wada, Y. Tanabe, Appl. Phys. Lett. 79 (2001) 3302.
[10] O. Tegus, E. Bruck, K.H.J. Buschow, F.R. de Boer, Nature (London) 415 (2002) 150.
[11] T. krenke, E. Duman, M. Acet, E.F. Wassermann, X. Moya, L. Manosa, A. Planes, Nat. Mater. 4 (2005) 450.
[12] A. de Campos, D.L. Rocco, A.M.G. Carvalho, L. Caron, A.A. Coelho, S. Gama, L.M. da Silva, F.C.G. Gandra, A.O. dos Santos, L.P. Cardoso, P.J. von Ranke, N.A. de Oliveira, Nat. Mater. 5 (2006) 802.
[13] N.K. Sun, W.B. Cui, D. Li, D.Y. Geng, F. Yang, Z.D. Zhang, Appl. Phys. Lett. 92 (2008) 072504.
[14] B.G. Shen, J.R. Sun, F.X. Hu, H.W. Zhang, Z.H. Chen, Adv. Mater. 21 (2009).
[15] H. Takeya, V.K. Pecharsky, K.A. Gschneidner Jr., J.O. Moorman, Appl. Phys. Lett. 64 (1994) 2739.
[16] Q. Zhang, B. Li, X.G. Zhao, Z.D. Zhang, J. Appl. Phys. 105 (2009) 053902.
[17] Q. Zhang, J.H. Cho, B. Li, W.J. Hu, Z.D. Zhang, Appl. Phys. Lett. 94 (2009) 182501.
[18] V.I. Nesterov, S.I. Reiman, I.N. Rozantsev, Fiz. Tverd. Tela 34 (1992) 270.
[19] N.N. Delyagin, V.I. Krylov, I.N. Rozantsev, J. Magn. Magn. Mater. 308 (2007) 74.
[20] S.K. Banerjee, Phys. Lett. 12 (1964) 16.
[21] A.H. Morrish, Physical Principles of Magnetism, John Wiley & Sons, Inc., New York, 1965, p. 470.
[22] V.K. Pecharsky, K.A. Gschneidner Jr., J. Appl. Phys. 86 (1999) 565.
[23] J.C.P. Campoy, E.J.R. Plaza, A.A. Coelho, S. Gama, Phys. Rev. B 74 (2006) 134410.
[24] M.E. Wood, W.H. Potter, Cryogenics 25 (1985) 667.
[25] T. Tohei, H. Wada, J. Magn. Magn. Mater. 280 (2004) 101.
[26] X.X. Zhang, F.W. Wang, G.H. Wen, J. Phys.: Condens. Matter 13 (2001) L747.